

# A Novel Mechanism of Late Gene Silencing Drives SV40 Transformation of Human Mesothelial Cells

Michele Carbone,<sup>1</sup> Antonio Pannuti,<sup>1</sup> Lei Zhang,<sup>1</sup> Joseph R. Testa,<sup>2</sup> and Maurizio Bocchetta<sup>3</sup>

<sup>1</sup>Thoracic Oncology Program, Cancer Center of Hawaii and Department of Pathology, University of Hawaii Medical School, Honolulu, Hawaii; <sup>2</sup>Human Genetics Program, Fox Chase Cancer Center, Philadelphia, Pennsylvania; and <sup>3</sup>Thoracic Oncology Program, Cardinal Bernardin Cancer Center, Loyola University Chicago, Maywood, Illinois

## Abstract

**Suppression of the late gene expression, usually by integration of the viral DNA into the host genome, is a critical step in DNA tumor virus carcinogenesis. SV40 induces high rates of transformation in infected primary human mesothelial cells in tissue culture, leading to the formation of immortal cell lines (SV40-transformed human mesothelial cell lines, S-HML). The studies described here were designed to elucidate the unusual susceptibility of primary human mesothelial cells to SV40 carcinogenesis. We found that S-HML contained wild-type, mostly episomal SV40 DNA. In these cells, the early genes that code for the viral oncogenes are expressed; at the same time, the synthesis of the late genes, capsid proteins, is suppressed and S-HML are not lysed. Late gene suppression is achieved through the production of antisense RNA molecules. These antisense RNA molecules originate in the early region of the SV40 circular chromosome and proceed in antisense orientation into the late gene region, leading to the formation of highly unstable double-strand RNA, which is rapidly degraded. Our results reveal a novel biological mechanism responsible for the suppression of late viral gene products, an important step in viral carcinogenesis in humans.** [Cancer Res 2008;68(22):9488–96]

## Introduction

SV40 is a DNA tumor virus capable of infecting and transforming human cells in tissue culture (1). SV40 transforms cells through the activities of its two major oncogenes: the large T antigen (Tag) and the small t antigen (tag; refs. 1, 2). The late region of the SV40 genome synthesizes the major capsid protein VP-1 and the capsid proteins VP-2 and VP-3, which together enable the SV40 DNA to be packaged into transmissible infectious particles (3).

SV40 infection of human cells has been studied mostly in fibroblasts (1, 4–6), which are permissive to SV40 replication, and infection leads to cell lysis (1, 4–6). Malignant transformation is a rare event, which starts under lytic conditions when the SV40 DNA becomes integrated into the host cell genome with expression of the early region that codes for the Tag and tag and with parallel lack of expression of the late region (5, 6). Foci of SV40-transformed fibroblasts can be established in tissue culture but usually enter crisis, and only ~5% of these foci can be established as immortal cell lines. Crisis is a period in which the cells become growth

arrested after an initial extension of their life span caused by a carcinogen, such as SV40. SV40-transformed fibroblast cell lines that emerge from the crisis express Tag and tag but do not produce infectious SV40 (5, 6).

Synthesis of Tag and tag takes place soon after infection (1). The SV40 Tag binds and inactivates numerous host proteins, including p53 and pRb, and transactivates several cellular promoters (1, 2, 7). In addition, the Tag-p53 complex acquires its own oncogenic activity because it binds to the insulin-like growth factor-I (IGF-I) promoter and causes the production and the release of IGF-I, which promotes malignant cell growth (8). Direct and indirect functions of Tag are modulated by the activity of tag, a protein that binds and inactivates cellular protein phosphatase 2A. Through this inhibition, tag reinforces mitogenic stimuli acting through the extracellular signal-regulated kinase pathway, leading to activator protein-1 activation (9, 10). Additional functions of the SV40 early gene products have been described after infection of primary human mesothelial cells (HM), including the induction of hepatocyte growth factor and consequent *c-Met* phosphorylation (11), induction of Notch signaling (12), etc.

Tag is also required for SV40 DNA replication (13) and transcription (8, 14). During replication of the SV40 DNA, late gene transcription takes place. This is initiated by a dual mechanism: Tag-mediated transcriptional induction (15) and titration of cellular transcriptional repressors at the late promoter (at the so-called +1 and +55 hormone-responsive elements in the late SV40 region) by the accumulating SV40 DNA molecules (16–18). During the late phase of SV40 infection, human cells are blocked in G<sub>2</sub> because of the activation of the checkpoint kinase Chk1 (19). Accumulation of SV40 late proteins overstimulates cellular poly(ADP-ribose) polymerase—causing cell necrosis (20) and the release of infectious SV40 into the extracellular space. New cells are infected, and the infection propagates until cells are lysed (*in vitro*) or until the immune system clears the infection (*in vivo*). Nevertheless, through unknown mechanisms, SV40 can establish latency in permissive monkey kidney cells *in vivo* (1) and possibly in MH cells, because ~5% to 10% of nonmalignant HM (pleural) biopsies tested were SV40-positive (6, 21, 22).

The undifferentiated nature of the mesothelial cells, a remnant of mesoderm, may account for some of their unusual characteristics, such as their high susceptibility to SV40 infection (23, 24), asbestos (25), and erionite (26) carcinogenesis and to the unique histologic and clinical features of mesotheliomas, the tumors that originate from these cells. SV40 causes mesotheliomas in hamsters (9, 27). Some tested human mesotheliomas were SV40-positive, although different studies reported different percentages of positivity (~0–60%; reviewed in refs. 5, 6, 28–32). These findings have caused a debate in the scientific community about the possible role of SV40 in the pathogenesis of human mesothelioma and other malignancies (1, 6, 28–32).

**Note:** Supplementary data for this article are available at Cancer Research Online (<http://cancerres.aacrjournals.org/>).

**Requests for reprints:** Michele Carbone, University of Hawaii Medical School, 651 Ilalo Street, BSB-231-H, Honolulu, HI 96813. Phone: 808-440-4596; Fax: 808-587-0790; E-mail: mcarbone@crch.hawaii.edu.

©2008 American Association for Cancer Research.  
doi:10.1158/0008-5472.CAN-08-2332

Although the role of SV40 in human mesotheliomas is still debated (32), there is general agreement among laboratories that, in tissue culture, HM are unusually susceptible to SV40 infection and malignant transformation (11, 23, 24, 33, 34). HM express high levels of wild-type p53 that binds to Tag and inhibits Tag-mediated SV40 replication (23). The oncogenic activities of Tag (1, 2, 7, 8, 11, 12) and the limited cell lysis lead to a rate of transformation of  $\sim 1/5,000$  SV40-infected mesothelial cells (S-HM), as measured by the number of tridimensional foci, compared with  $\sim 1/10^7$  to  $10^9$  rate of transformation observed in SV40-infected human fibroblasts (1, 11, 23, 24, 33, 34). Moreover, whereas  $<5\%$  of fibroblast-derived foci give rise to immortal cell lines,  $\sim 90\%$  of those derived from S-HM give rise to immortal SV40-transformed human mesothelial cell lines (S-HML; refs. 11, 12, 23, 35).

The studies described here were designed to investigate the genetic expression of SV40 in S-HM and S-HML and their possible relationship to the unusual susceptibility of HM to SV40-mediated malignant transformation. We show that, in SV40-infected HM, there is an active process of late gene silencing mediated by long, antisense late RNA molecules. This process coincides with HM transformation, and it is probably required for the maintenance of the transformed phenotype.

## Materials and Methods

**Cell culture and infections conditions.** HM and S-HML were cultured and infected as we described (23, 33). For details, see supplementary data.

**Antibodies, immunocytochemistry, and Western blot experiments.** These were as we described (23, 33), for details see supplementary data.

**Plasmid construction, luciferase, and RNA interference assays, fluorescence *in situ* hybridization, transfection, Northern blotting, and Southern blotting experiments.** These were according to standard procedures. For details, see supplementary data.

**Nuclear run-on experiments.** Nuclear run-on assays on  $5 \times 10^6$  nuclei purified from each sample were performed as described (36).

***In situ* hybridization.** *In situ* hybridizations were performed as described (37). For details, see supplementary data.

**SV40 late mRNAs half-life measurements.** SV40 late mRNAs half-life was determined by mRNA decay. This was assayed after exposure of cells to  $50 \mu\text{g/mL}$  of  $\alpha$ -amanitin (Sigma-Aldrich) at the time points specified. No reverse transcriptions of each sample were used as negative controls. VP-1 mRNA values were normalized for 28S rRNA amounts and plotted as percentage of the time 0 sample. See supplementary data for details and ref. 38.

**RNA polymerase II quantitative chromatin immunoprecipitation.** Chromatin immunoprecipitation (ChIP) was carried out as described in the ChIP kit protocol from Upstate Biotechnology, with minor modifications. See supplementary data and Supplementary Table S1 for details.

**Strand-specific quantitative reverse-transcriptase PCR.** Total RNA was extracted from S-HML1 cells using the Qiagen RNeasy kit, treated with Q-DNase (Promega), and reextracted using the same kit. (A graphic representation of the experimental procedure is provided in Supplementary Fig. S1.)

The RNA was reverse transcribed using the Superscript III RT from Invitrogen ( $2 \mu\text{g}$  of RNA/reaction at  $55^\circ\text{C}$  for 20 min) using 18 primers (in separate reactions) to synthesize cDNAs from sense and antisense RNAs derived from the early and late regions of the SV40 genome. The sequences of the primers used are listed in Supplementary Table S1.

To detect antisense late SV40 transcript using end-point reverse-transcriptase PCR (RT-PCR),  $2 \mu\text{g}$  of total RNA isolated from S-HML1 and S-HML4 were reverse transcribed using primer 5'-CCCCAAAAATGCTACAGTTGAC-3' (positions 2040–2062 of the SV40 genome). Reverse transcription reactions were then PCR amplified using primers 5'-GGGTGTTGGCCCTTGTGCAAAGC-3' (LA1) and 5'-CATGTCTGATCCCAGGAAGCTC-3' (LA2). Sense late gene transcripts were reverse

transcribed using primer 5'-AGTTGTGTTTGTCCAAACTATC-3' (positions 2581–2558 of the SV40 genome) and amplified with primers LA1 and LA2. Real-time PCR using SYBR green (Applied Biosystems) was performed according to standard protocols. Putative antisense early transcripts were reverse transcribed using either primer LA1 or 5'-ACCACAACCTAGAAATG-CAGTGAAAAA-3' (positions 2573–2598 of the SV40 genome), and the cDNA was amplified with the primers 5'-TTTATCAGCATTTCCTGGCTGTCTCC-3' and 5'-ACCTGTGGCTGAGTTTGTCTCA-3', which should have amplified a 188-bp DNA fragment (Supplementary Table S1) corresponding to positions 2881 to 3069 of the SV40 genome. We used SV40 strain 776 (1); no polymorphism was detected at the Tag carboxy terminus.

## Results

**Initial observations: S-HML express Tag and do not express VP-1.** Immunostaining experiments revealed that Tag was expressed in  $\sim 100\%$  of S-HM (data not shown and ref. 23) and in all S-HML ( $\sim 100\%$  of the cells in seven of seven tested cell lines; Fig. 1A). *In situ* hybridization experiments supported the immunostaining results because SV40 genomes were detected in the nuclei of most cells in each S-HML (Fig. 2C). Although  $\sim 100\%$  of the cells expressed Tag in both S-HM and S-HML, Western blot experiments indicated that the amounts of Tag were markedly elevated in S-HML compared with early-infected mesothelial cells (S-HM; Fig. 1C).

Instead, VP-1 staining was positive in  $\sim 100\%$  of S-HM from 48 hours to 2 weeks postinfection (Supplementary Fig. S2), but it was either completely negative (Fig. 1B) or mostly negative with rare positive staining cells ( $\sim 1/10^{5-6}$ ) in S-HML. Western blot analyses revealed high levels of VP-1 in S-HM soon after infection and low to undetectable levels in S-HML (Fig. 1D). These data were supported by electron microscopy. SV40 particles were readily detectable by electron microscopy in S-HM, as measured at 72 hours and 2 weeks postinfection, but were not detected in S-HML (data not shown; ref. 23). Nevertheless, all seven S-HML

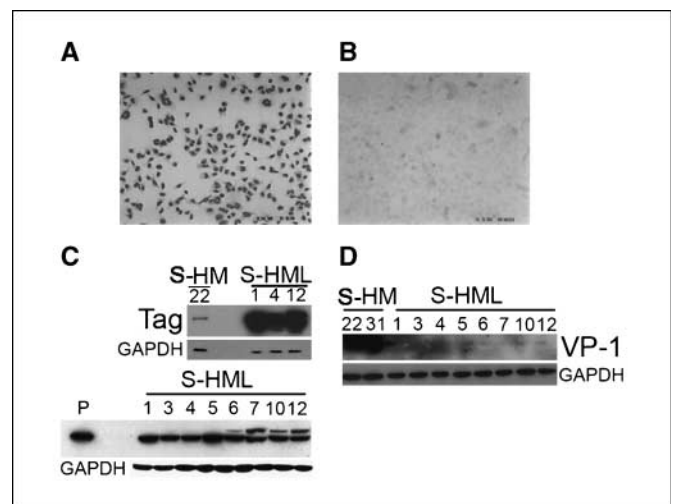


**Figure 1.** S-HML express SV40 early genes but do not express SV40 late genes. A and B, immunocytochemistry on S-HML1. Tag (A) and VP-1 (B) staining. Original magnification,  $100\times$ . Tag is uniformly expressed in these cells. VP-1 expression is undetectable. C and D, Western blot analysis of Tag (C) and VP-1 (D). In C, the amounts of Tag in S-HML are compared with those detected in S-HM 72 h after infection (top gel) and to  $0.25 \mu\text{g}$  of purified Tag (lane P, bottom gel). D, expression levels of VP-1 in S-HM 22 and S-HM 31 72 h after SV40 infection compared with VP-1 levels in different S-HML. Lane P,  $100 \mu\text{g}$  of total cell lysates were loaded in each lane. Glyceraldehyde-3-phosphate dehydrogenase is the loading control.

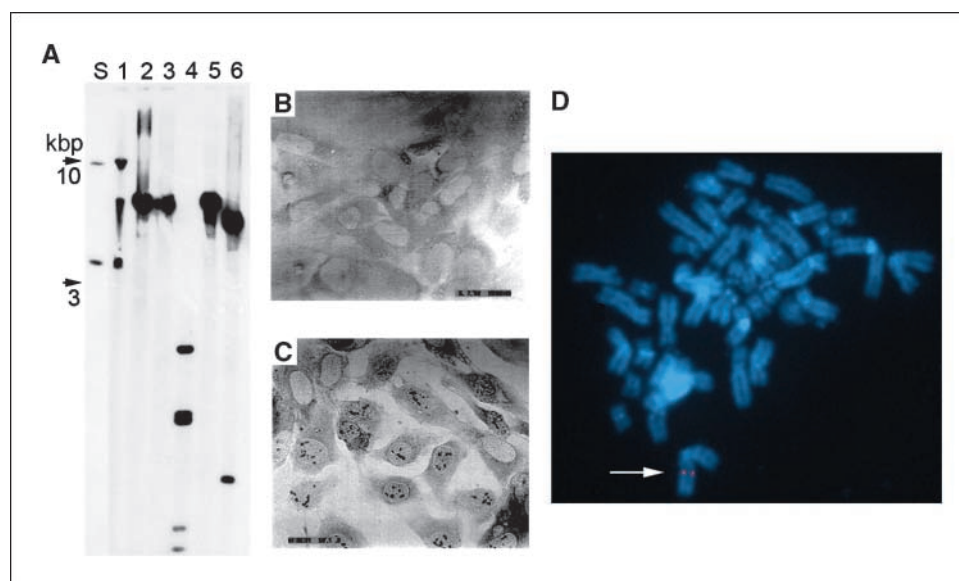


**Figure 2.** S-HML1 contains episomal SV40 genomes. Representative set of experiments (similar results were obtained in different S-HML). **A**, Southern blot performed on total DNA (10  $\mu$ g/lane) extracted from S-HML1. *Lane S*, 5 ng of purified, uncut SV40 DNA (the upper band  $\sim$ 10 kb corresponds to circular relaxed DNA, the lower band to linear DNA); *lane 1*, uncut S-HML1 genomic DNA (note the absence of high molecular weight DNA hybridizing with the SV40 probe); *lane 2*, *Bam*HI; *lane 3*, *Eco*RI; *lane 4*, *Hind*III; *lane 5*, *Kpn*I; *lane 6*, *Bsp*HI. Blots were hybridized with a  $^{32}$ P-labeled SV40 probe. *Bam*HI, *Eco*RI, and *Kpn*I have one restriction site within the SV40 genome, *Bsp*HI cuts twice, whereas *Hind*III produces the characteristic pattern shown in lane 4. Southern blot analysis was performed after 75 passages in tissue culture. DNA sequencing of SV40 genomes extracted from this clone indicated that cells contain wild-type, nonarchetypal SV40. **B** and **C**, *in situ* hybridization using biotinylated oligonucleotides with a random sequence (**B**) or complementary to SV40 (**C**). Because this technique identifies, on average,  $\sim$ 1/10 genomes copies (37), the occasional negative staining cells may contain  $<$ 10 copies of SV40. **D**, chromosomal localization of SV40 DNA sequences on metaphase spread from S-HML1 (passage 13) as determined by FISH. Note specific hybridization signals on a marker chromosome interpreted to be a 7;13 derivative chromosome. The photograph represents digitally enhanced, merged images of SpectrumOrange signals (arrow) and 4',6-diamidino-2-phenylindole-stained chromosomes; the latter is displayed in blue.

released low amounts of infectious SV40, because their tissue culture media caused vacuolization and lysis of monkey kidney cells (CV-1) 4 to 5 weeks after inoculation (compared with CV-1 infected at a multiplicity of infection of 1 per cell, in which extensive cell lysis was observed within a week). In summary, these data showed active SV40 production in S-HM up to 2 weeks postinfection and low to undetectable VP-1 expression, paralleled with low virus production, in S-HML in spite of the presence and expression of SV40 Tag in  $\sim$ 100% of the cells in each of these seven cell lines.

#### S-HML contain mostly episomal wild-type SV40 genomes.

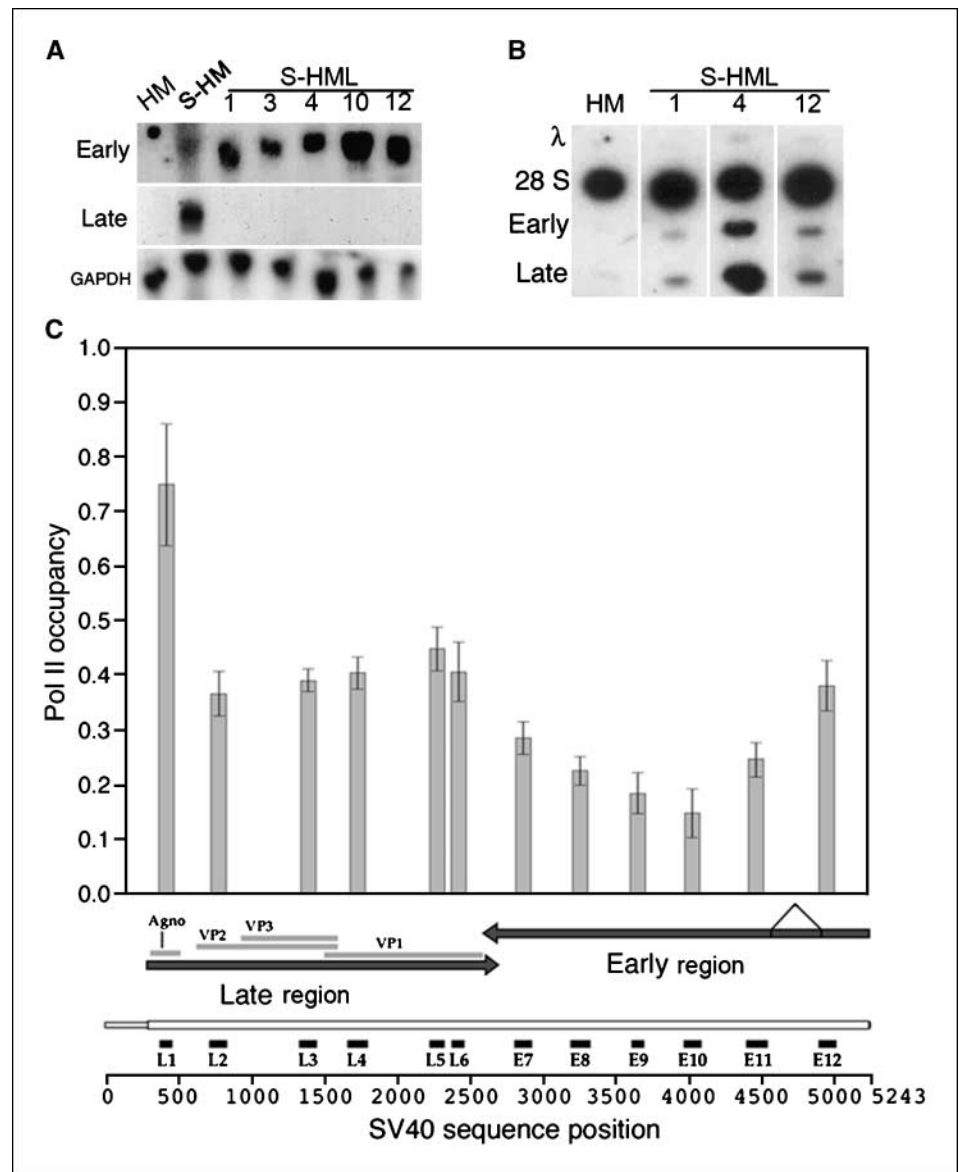
We expected that the disappearance of VP-1 in S-HML was caused by the integration of the SV40 DNA into the host genome with consequent disruption of the late coding regions. Southern blot analyses performed on total DNA extracted from S-HML did not detect integration of the SV40 DNA within the genomes of different S-HML. Instead, low molecular weight ( $\sim$ 5 kb), possibly episomal, SV40 DNA was detected (Fig. 2A). To reconcile these unexpected results with the integration hypothesis, we speculated that the pattern generated by the restriction analysis could have originated from the integration of SV40 DNA in multiple tandem repeats in a head-to-tail arrangement. Also, the absence of high molecular weight DNA might have been related to the possible inability of this DNA to enter the agarose gel. To test for the presence of "true" low molecular weight SV40 DNA, we extracted DNA from  $5 \times 10^6$  cells from seven different S-HML following a standard alkali/SDS procedure (a protocol used to extract plasmid DNA from *Escherichia coli*) and analyzed these DNAs by Southern blot hybridization. Comparisons of the amounts of extracted DNAs with known amounts of SV40 DNA indicated that different S-HML contained, on average,  $\sim$ 50 (S-HML1) and up to  $\sim$ 1,000 copies

(S-HML4, the cell line with more SV40 DNA) of SV40 DNA per cell (Supplementary Fig. S3). These results supported the presence of episomal SV40 in S-HML. At the same time, fluorescence *in situ* hybridization (FISH) showed that  $\sim$ 20% of metaphase spreads contained an about one to three copies of integrated SV40 per cell (Fig. 2D). FISH did not detect SV40 in the remaining 80% of cells in these cell lines. Because Tag immunostaining (Fig. 1A) and *in situ* DNA hybridization (Fig. 2B and C) revealed the presence of SV40 DNA in almost 100% of the S-HML, these results supported the interpretation that SV40 was present mostly as an episome inside S-HML, although a minor subpopulation of cells contained integrated SV40. This finding is in agreement with a recent report by K. Rundell, who found the presence of episomal SV40 in S-HML developed in her laboratory (34).

These initial set of data indicated that VP-1 capsid protein expression was suppressed in the vast majority of S-HML. In the 20% of cells containing integrated SV40, VP-1 suppression could have been caused by the disruption of the integrity of the late regions during the process of integration of SV40 into the host cell genome. But how was VP-1 capsid protein expression suppressed in the majority of S-HML containing episomal SV40 and expressing Tag?

**DNA sequence analyses.** We sequenced both the integrated and the episomal SV40 DNAs from S-HML1 and S-HML4 using procedures to separately isolate high and low molecular weight DNA. Two separate extractions were performed from each cell line, and the results were analyzed in parallel. To study the SV40 DNA sequences integrated into high molecular weight DNA, we used PCR analyses with primers that amplify the regulatory and the late SV40 regions, followed by DNA sequencing. We detected extensive

**Figure 3.** Transcription of the early and late genes in S-HML. **A**, Northern blot hybridization on 40  $\mu$ g of total RNA extracted from noninfected HM and S-HM 72 h after infection (lane 2) and from different S-HML. Note that 72 h after SV40 infection, HM express both early and late SV40 mRNAs. The 16S late mRNA, which encodes VP-1, is shown; the 19S mRNA, which codes for the other SV40 late proteins (48). Instead, S-HML express only early mRNA, but late mRNAs are not detectable by Northern blot in these same cells. **B**, nuclear run-on performed on purified nuclei from HM and three different S-HML. The dot seen on the top left corner likely represents nonspecific binding of the probe to the filter. *Early*, 5  $\mu$ g of double-stranded, alkali-denatured early probe; *late*, 5  $\mu$ g of double-stranded, alkali-denatured late probe;  $\lambda$ , 5  $\mu$ g alkali-denatured  $\lambda$ DNA digested with *Hind*III; *28S*, 5  $\mu$ g of double-stranded, alkali-denatured PCR product of the 28S rRNA gene. S-HML nuclei synthesize approximately 3 $\times$  more late than early transcripts. **C**, RNA Pol II occupancy along the SV40 genome in S-HML1. Pol II occupancy was determined by quantitative PCR after ChIP with a rabbit polyclonal antibody raised against the NH<sub>2</sub> terminus of the large subunit of Pol II. The PCR amplicons are reported below a schematic map of the SV40 genome in a linear form (nucleotide numbering is from Genbank accession AF316139). Averaged values ( $\pm$ SD) from three independent immunoprecipitations are reported on the horizontal axis, expressed as percentage of input chromatin immunoprecipitated by Pol II antibody. As expected, Pol II density is higher in proximity of the early and late transcriptional start sites compared with the rest of each transcriptional unit. On the average, Pol II occupancy seems higher on the late region than on the early region.



rearrangements in the integrated DNA. For example, DNAs from both cell lines contained insertions of DNA sequences from the early region in sense or antisense orientation within the sequences of the SV40 regulatory and late regions (not shown). The finding that these rearranged sequences were not detected by Southern blot hybridization (Fig. 2) supports the FISH results, showing that integrated SV40 represents a minority of the SV40 DNA present in S-HML.

To study episomal SV40, low molecular weight SV40 DNA was cloned into pUC21, and we sequenced the DNAs of four independent clones. The results showed the presence of wild-type SV40 DNA identical to the SV40 strain 776 used to transform these cells. These findings did not support the hypothesis that DNA mutations within the SV40 late region caused the lack of VP-1 expression.

**VP-1 mRNA is undetectable in S-HML by Northern blot analyses.** Abrogation of VP-1 expression seemed to coincide with morphologic transformation (i.e., the appearance of flat foci) and

was maintained throughout culturing of S-HML (see Supplementary Fig. S1).

The steady-state levels of expression of the early and late mRNA were measured by Northern blot in both early-infected S-HM and S-HML. At 72 hours after SV40 infection, S-HM expressed detectable amounts of early mRNA and apparently larger amounts of late mRNA (an indication of a heterogeneous cell population, in which some S-HM are in the early phase of SV40 infection whereas other S-HM are in the late phase). Instead, S-HML expressed higher amounts of early SV40 mRNA compared with S-HM, but the late mRNAs were undetectable (Fig. 3A). These results closely matched the protein studies (Fig. 1). The absence of late mRNA in S-HML suggested that transcription at the SV40 late promoter was suppressed.

To test this hypothesis, we conducted a number of experiments, which are briefly summarized below (see also the supplementary data). Bisulfite sequencing showed no methylation of the SV40 regulatory region up to the +55 transcription regulatory element.

In parallel, aza-dC and thicostatin A treatment of S-HML did not rescue VP-1 expression in S-HML. Likewise, treatment of different S-HML with thyroid, retinol, and different estrogen hormones failed to rescue VP-1 expression in these cells. Treatment of CV-1 cells with these same hormones induces transcription of the late genes during the early phase of viral infection (16, 17). Because S-HML seemed to overexpress retinoid X receptor  $\alpha$  and thyroid hormone receptor  $\alpha$  (the latter are two known transcriptional repressors of the SV40 promoter; refs. 17, 18), we used RNA interference (RNAi) approaches to artificially down-regulate these proteins, yet we could not rescue VP-1 expression in S-HML (Supplementary Fig. S4). In summary, these experiments did not support the hypothesis that late gene silencing in S-HML was caused by DNA methylation or by known transcriptional repressors of the SV40 late promoter.

**SV40 late promoter is transcriptionally active in S-HML.** We cloned firefly luciferase under the control of the late promoter [two different constructs: (a) luciferase was under the control of the entire SV40 regulatory region, including the +1 regulatory element; (b) luciferase was placed downstream from the late intron, therefore including the +1 and the +55 regulatory elements]. These plasmids were transfected in three different S-HML and three different primary HM, and reporter gene activity was evaluated by a luminometer. Both the +1 Luc and +55 Luc (see supplementary data) gave background readings (10–30 light units) when transfected into HM. Cell lysates from S-HML transfected with +1 Luc gave  $>1 \times 10^5$  light units (i.e., maximum instrumental readings). S-HML transfected with the +55 Luc plasmid gave readings of 2 to  $5 \times 10^4$  light units (data not shown). These data indicated that luciferase, under the control of the SV40 late promoter, was actively expressed in S-HML, disproving the hypothesis of transcriptional repression of the late SV40 promoter.

We challenged the reporter assay experiments by measuring the rate of transcription at the early and late promoters in S-HML through nuclear run-on experiments. The results showed that nuclei extracted from different S-HML transcribed, on average,  $3 \times$  more late than early transcripts (Fig. 3B). Furthermore, quantitative ChIP experiments showed that RNA polymerase II (Pol II) was present on both the early and late regions of the SV40 genome in S-HML1 (Fig. 3C; same results were obtained in S-HML4, not shown). As expected, Pol II density was higher in the proximity of the early and late transcriptional start sites compared with the rest of each transcriptional unit. In agreement with the results from the run-on experiments, we found that, on

average, Pol II occupancy on the SV40 genome was higher on the late region than on the early region, with a maximum peak at the initiation of transcription of the late region (Fig. 3C). Together, these results indicated that the late SV40 promoter was actively transcribed in S-HML.

**SV40 late transcripts have a shorter half-life in S-HML compared with early-infected S-HM.** To study this paradox (active transcription at the SV40 late promoter that resulted in nondetectable steady-state amounts of the late mRNA in S-HML), we measured the half-life of the late transcripts in S-HM 72 hours after infection and in S-HML. We performed mRNA decay assays using  $\alpha$ -amanitin to inhibit RNA Pol II, followed by real-time RT-PCR to detect late transcripts. Precisely, the half-life measured was that of the 84-nucleotide-long fragment of the VP-1 mRNA at the 3' terminal portion (positions 2009–2093; see supplementary data for details). In Fig. 4, we show the summary of the SV40 late RNA decay experiments performed on four different S-HM 72 hours after SV40 infection (Fig. 4A) and on two different S-HML (Fig. 4B). SV40 late mRNAs displayed a half-life  $>5$  hours in S-HM. Instead, in S-HML, the SV40 late RNA half-life was only 30 minutes. The bimodal curve of RNA decay in S-HML (Fig. 4; a steep decay in the first 30 minutes followed by a less pronounced decay similar to that observed in S-HM) suggested that 30 minutes after  $\alpha$ -amanitin administration, which is approximately the time required to inhibit RNA Pol II, the late RNA in S-HML became more stable. This unexpected finding suggested that RNA Pol II-dependent transcription was required for late mRNA destabilization. We investigated this hypothesis.

**S-HML transcribe antisense late RNA.** Continuous degradation of late mRNA in S-HML could be maintained in these cells if an active mechanism of RNAi takes place, either mediated by specific microRNAs (miRNA) or by long antisense RNA duplexes. A putative miRNA precursor that could target the late genes has been identified in the early SV40 region, positions 29 to 5201 (39). However, the functionality of such miRNA precursor has been disproved (39). Instead, there is an miRNA precursor in the late transcripts that promotes degradation of the early transcripts during the late phase of SV40 infection (39). To study whether miRNA processing caused the rapid degradation of late transcripts, we down-regulated nRnase III Droscha (40) using RNAi. This strategy did not rescue VP-1 mRNA expression in S-HML (Supplementary Fig. S5).

Next, we considered the possibility that long complementary RNA could have mediated late gene silencing in S-HML (41).

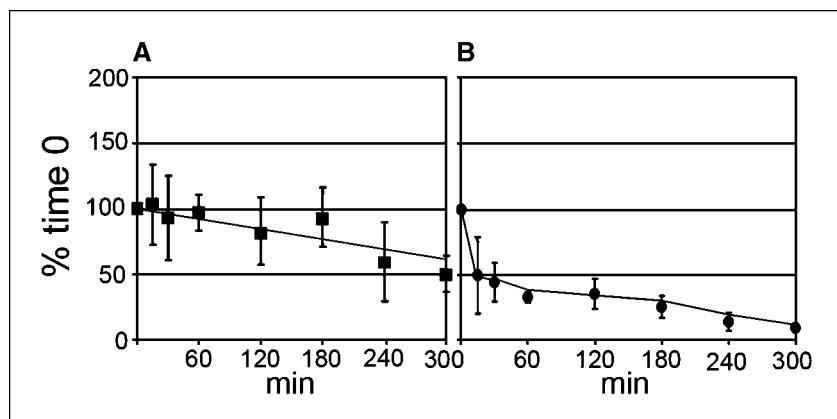
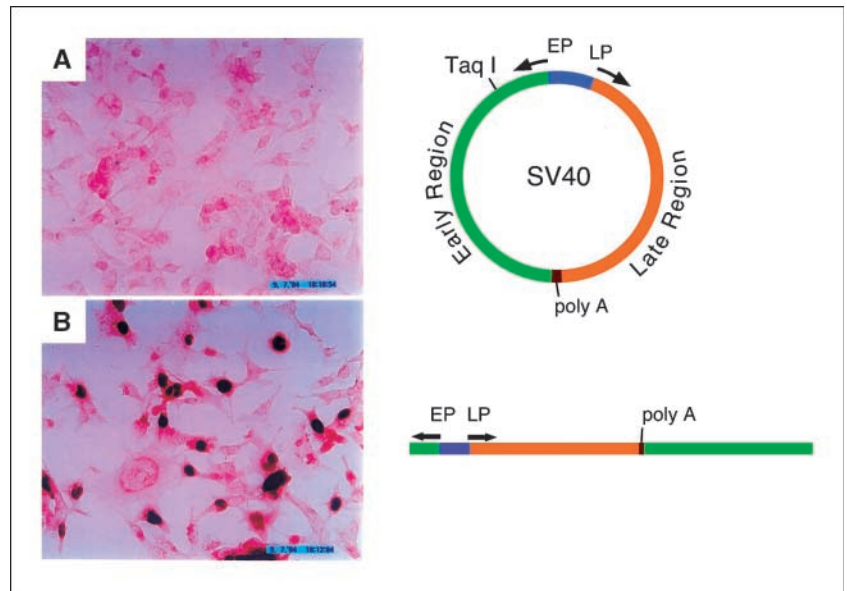


**Figure 4.** Shortened SV40 late mRNA half-life in S-HM (A) compared with early infected S-HML (B). mRNA decay experiments in four different HM 72 h after SV40 infection in two S-HML. The experiments were repeated thrice for both, S-HML1 and S-HML4.

**Figure 5.** Linearized SV40 DNA rescues VP-1 synthesis in a fraction of transfected S-HML. At 24 h after transfection, cells were assayed by immunocytochemistry. **A**, lack of VP-1 expression in S-HML1 24 h after electroporating 10  $\mu$ g of circular SV40 DNA. The arrows on the SV40 map represent the direction of transcription from the early promoter (EP) and late promoter (LP). The region containing the early and late polyadenylation sites is indicated as poly(A). **B**, VP-1 immunostaining of S-HML1 24 h after electroporating 10  $\mu$ g of Taq I-digested SV40 DNA. Note VP-1 expression in these cells. As expected, reactivation is transient and disappears 3 to 5 d after transfection. Similar results were obtained in S-HML4.



Antisense late SV40 RNAs could be generated if transcription of the SV40 early genes would extend beyond 180° around the SV40 circular chromosome (Fig. 5). To begin testing the hypothesis that transcription beyond the polyadenylation signal into the late region in antisense orientation to the late mRNA could have accounted for late gene silencing in S-HML, we performed the following experiment. Two aliquots of 20  $\mu$ g of purified SV40 DNA were handled in parallel. One aliquot was digested with Taq I, which cuts the early region of the SV40 genome at position 4740. The resulting linear molecule contained the regulatory region that may have driven transcription of truncated early mRNAs (including the putative miRNA precursor at positions 29–5201), whereas the late promoter could have driven the transcription of the entire late mRNAs. The other SV40 DNA aliquot was mock-digested and purified in parallel to the digested aliquot. Transfection of S-HML with circular SV40 did not induce VP-1; instead, transfection with the linearized SV40 DNA rescued VP-1 expression in 10% to 30% of transfected cells (Fig. 5). Therefore, by linearizing the SV40 DNA and, thus, preventing the putative formation of an antisense message originating from the early region, we could rescue VP-1 expression in a fraction of the transfected cells.

To test the existence of late antisense transcripts, we built a transcriptional map of the SV40 genome in S-HML1 through strand-specific RT followed by quantitative PCR (see Supplementary Materials and Methods, Supplementary Table S1, and Supplementary Fig. S5 for a schematic outline of the experimental strategy). We used six primer couples for the late SV40 region and three primer couples for the early SV40 region. As shown in Fig. 6, we found that early region transcripts are preponderantly represented by sense RNAs. On the other hand, we detected comparable levels of both sense and antisense late transcripts (Fig. 6). Antisense late RNA sequences were detected for the entire late transcription unit. This result is consistent with a scenario wherein Pol II, transcribing the early region, reads through the early polyadenylation signal and then proceeds transcribing into the late region, thus generating a long late antisense RNA. This late antisense RNA seems linked to the destabilization of the late mRNAs (Fig. 4). In conclusion, a silencing mechanism mediated by

long antisense RNA reconciles the results, showing an active SV40 late promoter in S-HML with the lack of mature late mRNAs and late viral protein synthesis.

This phenomenon seems to be established early in the process of S-HM transformation. Two weeks after SV40 infection, morphologically transformed flat foci did not express VP-1 by immunohistochemistry whereas the surrounding S-HM did express VP-1 (Supplementary Fig. S2). SV40 late gene silencing was also observed in primary human brain cells (astrocytes) in tissue culture upon SV40-mediated transformation (Supplementary Fig. S6).

## Discussion

Studying the process of SV40-mediated transformation of HM, we discovered a novel biological mechanisms that leads to the suppression of viral late gene products. This mechanism is based on the generation of antisense mRNA molecules to repress late gene expression. We found that S-HML express the early genes that are responsible for SV40-mediated transformation but do not synthesize the late gene products that are required for viral DNA packaging (3) and promotion of host necrosis (20). Because the late gene products are not synthesized in S-HML, episomal SV40 does not cause cell lysis. Therefore, there is no selective pressure for integration of SV40 into the host cell genome, and the SV40 chromosome remains mostly episomal even after prolonged passage in tissue culture. Our results provide a mechanistic explanation to the paradox that episomal SV40 does not cause extensive cell lysis in HM and that, instead, the presence of episomal SV40 leads to a very high rate of malignant transformation ( $\sim 1/5,000$  infected cells) compared with the rate of transformation observed in human fibroblasts ( $1/10^{7-9}$  infected cells).

Although no late mRNA was detected in S-HML, reporter assays, run-on experiments, and Pol II ChIP assays revealed that the late SV40 regions were actively transcribed. However, RNA decay assays indicated that the late mRNA stability was significantly decreased in S-HML compared with early-infected S-HM, suggesting that the late mRNA was being rapidly degraded (Fig. 4).

We hypothesized that a putative antisense RNA could be generated if the early transcripts extended beyond the early polyadenylation signal into the late region, thus generating double-stranded RNA molecules, which are targets for Dicer-mediated degradation (42, 43). This hypothesis was supported by the observation that Taq I linearized SV40 genomes transiently rescued VP-1 synthesis in S-HML in some of the transfected cells. These DNA molecules can only generate late mRNA and short, truncated early transcripts but cannot generate late antisense molecules (Fig. 5). To detect the possible presence of the putative antisense late transcripts in S-HML, we designed a strand-specific quantitative RT-PCR analysis (see Supplementary Fig. S5 for an outline of the experimental approach). We found that sense RNA is predominantly detected among RNA molecules corresponding to the SV40 early region. On the other hand, in most of the SV40 late region, we detected comparable amounts of both sense and antisense RNAs. The late VP-1 mRNA was not detectable by Northern blot, and the overall level of late RNA measured by quantitative RT-PCR was lower than early RNA level, indicating fragmented late sense transcripts (Fig. 6). Together, these results are consistent with our hypothesis that, in S-HML, long, double-stranded late RNA molecules mediate SV40 late gene silencing. Considering that the early mRNA is properly processed (Fig. 3), our findings suggest that there is uncoupling between the polyadenylation and termination complexes (44), leading to the production of an intact early message, whereas the polymerase remains on the DNA template and proceeds on producing RNA in antisense orientation to the late message. The relatively low amount of late antisense, detected by the L5 and L6 primers soon after the polyadenylation site, seems to support this interpretation. In fact, at the 3' end of the late region, the ratio antisense/sense drops at values of ~11% and 9% for amplicons L5 and L6 (Fig. 6).

Late gene silencing seems to be an early event in SV40-mediated transformation of S-HM (see Supplementary Fig. S1), which persists

during passage in tissue culture. In preliminary experiments aimed at determining whether late gene silencing was observed in other cell types, we have observed this effect in primary human astrocytes infected in tissue culture with SV40. Similarly with S-HML, 2 months postinfection, SV40-transformed human astrocytes showed a progressive reduction of VP-1 expression and a parallel increase in Tag expression (Supplementary Fig. S6). Brain cells are also very susceptible to SV40 carcinogenesis (1). It seems possible that silencing of SV40 late gene expression may favor malignant transformation by reducing the risk of SV40 late gene-induced cell necrosis (20).

In some cell types, expression of long double-stranded RNA molecules activates the IFN response with consequent stimulation of protein kinase R (PKR), an event that leads to general translational repression in mammalian cells and apoptosis (45). In cells where long double-stranded RNA molecules do not elicit PKR activation (such as S-HML), expression of long antisense RNA duplexes elicits degradation of the target mRNA because each individual duplex can generate an undefined number of small interfering RNA; therefore, there is no need for a 1:1 ratio between the target mRNA and its antisense molecule because one duplex can generate numerous miRNAs targeting the sense RNA (41).

Infected fibroblasts produce large amounts of SV40 and undergo SV40-promoted cell necrosis. Thus, it is possible that, in fibroblasts and in other permissive cell types, late gene silencing mediated by antisense late RNA either does not take place or is a short-lived phenomenon insufficient to repress VP1-3 production. Experiments are in progress to address this hypothesis.

DNA tumor viruses transformation is often associated with integration of the viral DNA into the host cell genome (31, 46); thus, the finding that SV40 was prevalently episomal in S-HML was unexpected. Episomal SV40 in cancer cells is disadvantageous because viral late proteins can be synthesized and these proteins, which are not required for cellular transformation, promote

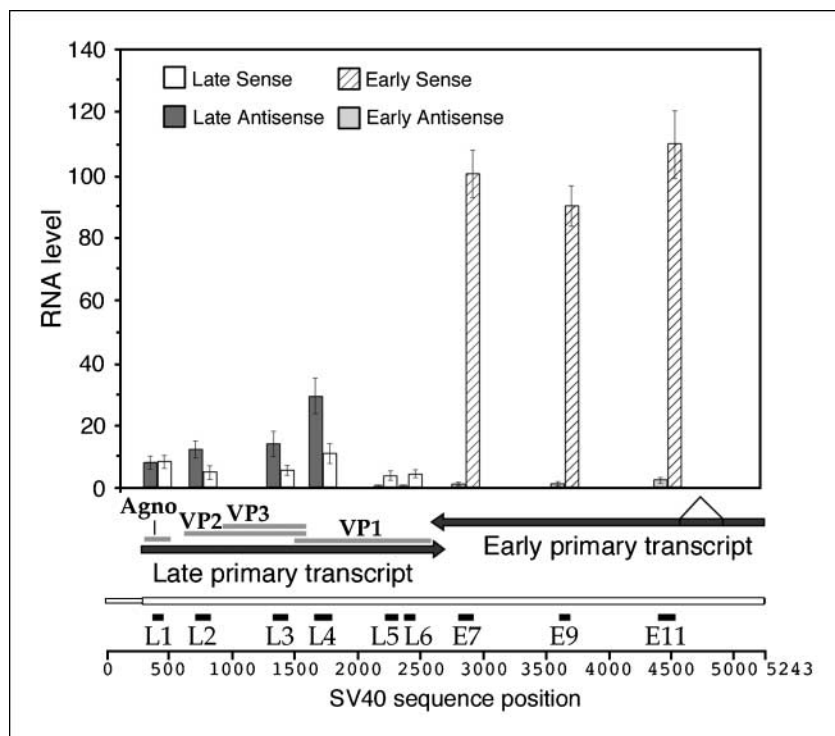


**Figure 6.** Transcriptional map of the SV40 genome in S-HML1 shows the presence of late antisense transcripts. RNA was measured by strand-specific reverse transcriptase followed by quantitative PCR. The PCR amplicons are reported below a schematic map of the SV40 genome in linear form (nucleotide numbering is from Genbank AF316139\*). Average values ( $\pm$ SD) were calculated from four quantitative PCR runs of samples derived from three independent strand-specific reverse transcriptase experiments. In the graph, the average value of sense RNA from the early region (amplicons E7, E9 and E11) is set to 100. The amplified fragments from the early region are almost exclusively from sense RNA. Instead, comparable levels of both sense and antisense amplicons are generated from the late region (<http://www.ncbi.nlm.nih.gov/Genbank/GenbankOverview.html>).

necrosis (20). Southern blot experiments revealed only (or prevalently) low molecular weight SV40 DNA in S-HML. Initially, we thought that these results were caused by the head-to-tail integration of multiple copies of SV40 into the host cell DNA. Subsequent experiments did not support this interpretation: large amounts of episomal SV40 were isolated using procedures optimized to extract plasmid DNA from bacteria (thus excluding high molecular weight DNA). FISH experiments revealed the presence of integrated SV40 in only 10% to 20% of cells in S-HML (Fig. 2D); however, most or all S-HML expressed SV40 Tag (Fig. 1) and contained SV40 DNA (Fig. 2B). Also, an extensive review of the literature did not identify any manuscript reporting the presence of perfect tandem repeats of SV40 integrated into human cells (perfect head-to-tail configuration would be required to produce the pattern seen in Fig. 2A). Therefore, the evidence supports the interpretation that S-HML contain episomal SV40, although a fraction of the cells also contain integrated SV40 DNA. Our findings in S-HML share some similarities with the EBV-associated malignancies in which, although the infection in the tumor cells is latent and does not produce virus, viral genes are expressed in all tumor cells (31). Thus, similar with EBV-associated malignancies (31), SV40-associated malignancies (6) may be susceptible to the influence of the immune system as the recent data seem to suggest (47).

The data presented here and previous results (23, 24) suggest the following model to account for the unusual susceptibility of HM to SV40-mediated transformation. The high endogenous levels of p53 present in HM bind Tag and slow down SV40 replication early during infection, thus preventing cell lysis (23). Subsequently, the generation of long antisense late transcripts prevents capsid protein production and, thus, viral particles formation and SV40 late gene protein-promoted cell necrosis. This allows SV40 to remain episomal without causing cell lysis, whereas the expression of the SV40 early genes causes HM malignant transformation.

## Disclosure of Potential Conflicts of Interest

No potential conflicts of interest were disclosed.

## Acknowledgments

Received 6/18/2008; revised 8/28/2008; accepted 9/2/2008.

**Grant support:** National Cancer Institute grants R01-CA092657, R01-CA106567, PO1-CA114047-0A1 (M. Carbone), ACS-RSG05-077-01-MBC (M. Bocchetta), and NIH P30-CA006927-46 (J.R. Testa) from the NCI and an appropriation from the Commonwealth of Pennsylvania.

The costs of publication of this article were defrayed in part by the payment of page charges. This article must therefore be hereby marked *advertisement* in accordance with 18 U.S.C. Section 1734 solely to indicate this fact.

We thank Drs. G. Gaudino, W. El Shamy, and H. Yang for the critical reading of the manuscript, J. Rudzinski and M.A. DeMarco for technical assistance, and Dr. D. Koubi for assistance with the FISH analyses.

## References

- Butel JS, Lednický JA. Cell and molecular biology of simian virus 40: implications for human infections and disease. *J Natl Cancer Inst* 1999;91:119–34.
- Testa JR, Giordano A. SV40 and cell cycle perturbations in malignant mesothelioma. *Semin Cancer Biol* 2001;11:31–8.
- Gordon-Shaag A, Ben-Nun-Shaul O, Roitman V, Yosef Y, Oppenheim A. Cellular transcription factor Sp1 recruits simian virus 40 capsid proteins to the viral packaging signal, *ses*. *J Virol* 2002;76:5915–24.
- O'Neill FJ, Carney H, Hu Y. Host range analysis of simian virus 40, BK virus and chimaeric SV40/BKV: relative expression of large T-antigen and Vp1 in infected and transformed cells. *Dev Biol Stand* 1998;94:191–205.
- Ozer HL, Banga SS, Dasgupta T, et al. SV40-mediated immortalization of human fibroblasts. *Exp Gerontol* 1996;31:303–10.
- Gazdar AF, Butel JS, Carbone M. SV40 and human tumours: myth, association or causality? *Nat Rev Cancer* 2002;2:957–64.
- Ali SK, DeCaprio JA. Cellular transformation by SV40 large T antigen: interaction with host proteins. *Semin Cancer Biol* 2001;11:15–21.
- Bocchetta M, Elias S, DeMarco MA, Rudzinski J, Zhang L, Carbone M. The SV40 large T Antigen-p53 complexes bind and activate the insulin-like growth factor-1 promoter stimulating cell growth. *Cancer Res* 2008;68:1022–9.
- Kroczyńska B, Cutrone R, Bocchetta M, et al. Crocidolite asbestos and SV40 are cocarcinogens in human mesothelial cells and in causing mesothelioma in hamsters. *Proc Natl Acad Sci U S A* 2006;103:14128–33.
- Rundell K, Parakati R. The role of the SV40 ST antigen in cell growth promotion and transformation. *Semin Cancer Biol* 2001;11:5–13.
- Cacciotti P, Libener R, Betta P, et al. SV40 replication in human mesothelial cells induces HGF/Met receptor activation: a model for viral-related carcinogenesis of human malignant mesothelioma. *Proc Natl Acad Sci U S A* 2001;98:12032–7.
- Bocchetta M, Miele L, Pass HI, Carbone M. Notch-1 induction, a novel activity of SV40 required for growth of SV40-transformed human mesothelial cells. *Oncogene* 2003;22:81–9.
- Fanning E, Knippers R. Structure and function of simian virus 40 large tumor antigen. *Annu Rev Biochem* 1992;61:55–85.
- Pipas J, Levine A. Role of T antigen interactions with p53 in tumorigenesis. *Semin Cancer Biol* 2001;11:23–30.
- Keller JM, Alwine JC. Activation of the SV40 late promoter: direct effects of T antigen in the absence of viral DNA replication. *Cell* 1984;36:381–9.
- Zuo F, Kraus RJ, Gulick T, Moore DD, Mertz JE. Direct modulation of simian virus 40 late gene expression by thyroid hormone and its receptor. *J Virol* 1997;71:427–36.
- Zuo F, Mertz JE. Simian virus 40 late gene expression is regulated by members of the steroid/thyroid hormone receptor superfamily. *Proc Natl Acad Sci U S A* 1995;92:8586–90.
- Wiley SR, Kraus RJ, Zuo F, Murray EE, Loritz K, Mertz JE. SV40 early-to-late switch involves titration of cellular transcriptional repressors. *Genes Dev* 1993;7:2206–19.
- Okubo E, Lehman JM, Friedrich TD. Negative regulation of mitotic promoting factor by the checkpoint kinase chk1 in simian virus 40 lytic infection. *J Virol* 2003;77:1257–67.
- Gordon-Shaag A, Yosef Y, Abd El-Latif M, Oppenheim A. The abundant nuclear enzyme PARP participates in the life cycle of simian virus 40 and is stimulated by minor capsid protein VP3. *J Virol* 2003;77:4273–82.
- Shivapurkar N, Wiethage T, Wistuba II, et al. Presence of simian virus 40 sequences in malignant mesotheliomas and mesothelial cell proliferations. *J Cell Biochem* 1999;76:181–8.
- Galateau-Salle F, Bidet PH, Iwatsubo Y, et al. SV40-like DNA sequences in pleural mesothelioma, bronchopulmonary carcinoma, and non-malignant pulmonary diseases. *J Pathol* 1988;184:252–7.
- Bocchetta M, Di Resta I, Powers A, et al. Human mesothelial cells are unusually susceptible to simian virus 40-mediated transformation and asbestos cocarcinogenicity. *Proc Natl Acad Sci U S A* 2000;97:10214–9.
- Yu J, Boyapati A, Rundell K. Critical role for SV40 small-t antigen in human cell transformation. *Virology* 2001;290:192–8.
- Yang H, Bocchetta M, Kroczyńska B, et al. TNF- $\alpha$  inhibits asbestos-induced cytotoxicity via a NF- $\kappa$ B-dependent pathway, a possible mechanism for asbestos-induced oncogenesis. *Proc Natl Acad Sci U S A* 2006;103:10397–402.
- Pass HI, Vogelzang N, Hahn SM, Carbone M. Malignant pleural mesothelioma. In: De Vita VT, Hellman S, Rosenberg SA, editors. *Cancer: principles and practice of oncology*. Philadelphia: Lippincott Williams and Wilkins; 2005. p. 1687–715.
- Cicala C, Pompetti F, Carbone M. SV40 induces mesotheliomas in hamsters. *Am J Pathol* 1993;142:1524–33.
- Stratton K, Almario DA, McCormick M, editors. SV40 contamination of polio vaccine and cancer. IOM Report. In: *Immunization safety review*. Washington, DC: The National Academies Press; 2002. p. 19–84.
- Klein G, Powers A, Croce C. Association of SV40 with human tumors. *Oncogene* 2002;21:1141–9.
- Wong M, Pagano JS, Schiller JT, Tevethia SS, Raab-Traub N, Gruber J. New associations of human papillomavirus, Simian virus 40, and Epstein-Barr virus with human cancer. *J Natl Cancer Inst* 2002;94:1832–6.
- Pagano JS, Blaser M, Buendia MA, et al. Infectious agents and cancer: criteria for a causal relation. *Semin Cancer Biol* 2004;14:453–71.
- Carbone M, Albelda SM, Broaddus VC, et al. Eighth International Mesothelioma Interest Group. *Oncogene* 2007;26:6959–67.
- Carbone M, Burck C, Rdzanek M, Rudzinski J, Cutrone R, Bocchetta M. Different susceptibility of human mesothelial cells to polyomavirus infection and malignant transformation. *Cancer Res* 2003;63:6125–9.
- Fahrback KM, Katzman RB, Rundell K. Role of SV40 ST antigen in the persistent infection of mesothelial cells. *Virology* 2008;370:255–63.

35. Foddiss R, De Rienzo A, Broccoli D, et al. SV40 infection induces telomerase activity in human mesothelial cells. *Oncogene* 2002;21:1434-42.
36. Schilling LJ, Farnham PJ. Inappropriate transcription from the 5' end of the murine dihydrofolate reductase gene masks transcriptional regulation. *Nucleic Acids Res* 1994;22:3061-8.
37. Nuovo GJ. Diagnosis of human papillomavirus using *in situ* hybridization and *in situ* polymerase chain reaction. In: Aquino de Muro M, Rapley R, editors. *Methods in Molecular Biology: gene probes, principles and protocols*. Totowa: Humana Press; 2002. p. 113-36.
38. Yajima T, Yagihashi A, Kameshima H, et al. Quantitative reverse transcription-PCR assay of the RNA component of human telomerase using the Taq-Man fluorogenic detection system. *Clin Chem* 1998;44:2441-5.
39. Sullivan CS, Grundhoff AT, Tevethia S, Pipas JM, Ganem D. SV40-encoded microRNAs regulate viral gene expression and reduce susceptibility to cytotoxic T cells. *Nature* 2005;435:682-6.
40. Gregory RI, Yan KP, Amuthan G, et al. The Microprocessor complex mediates the genesis of microRNAs. *Nature* 2004;432:235-40.
41. Tran N, Raponi M, Dawes IW, Arndt GM. Control of specific gene expression in mammalian cells by co-expression of long complementary RNAs. *FEBS Lett* 2004;573:127-34.
42. Billy E, Brondani V, Zhang H, Müller U, Filipowicz W. Specific interference with gene expression induced by long, double-stranded RNA in mouse embryonal teratocarcinoma cell lines. *Proc Natl Acad Sci U S A* 2001;98:14428-33.
43. Knight SW, Bass BL. A role for the RNase III enzyme DCR-1 in RNA interference and germ line development in *Caenorhabditis elegans*. *Science* 2001;293:2269-71.
44. Gromak N, West S, Proudfoot NJ. Pause sites promote transcriptional termination of mammalian RNA polymerase II. *Mol Cell Biol* 2006;26:3986-96.
45. Clemens MJ. PKR-a protein kinase regulated by double-stranded RNA. *Int J Biochem Cell Biol* 1997;29:945-9.
46. Feng H, Shuda M, Chang Y, Moore PS. Clonal integration of a polyomavirus in human Merkel cell carcinoma. *Science* 2008;319:1096-100.
47. Serman DH, Recio A, Carroll RG, et al. A Phase I clinical trial of single dose intrapleural IFN- $\beta$  gene transfer for malignant mesothelioma and metastatic pleural effusions: high rate of antitumor immune responses. *Clin Cancer Res* 2007;13:4456-66.
48. Cole CN. Polyomaviruses. In: Fields BN, Knipe DM, Howley PM, editors. *Fields Virology*. Philadelphia: Lippincott-Raven Publishers; 1996. p. 1997-2043.